

## Exploration of the geothermal filed in the eastern Phlegrean Fields caldera for sustainability analysis of low-middle temperatures exploitation

Iorio Marina<sup>1</sup>, Carotenuto Alberto<sup>3</sup>, Cavuoto Giuseppe<sup>1</sup>, Corniello Alfonso<sup>2</sup>, Di Fiore Vincenzo<sup>1</sup>, Fedi Maurizio<sup>2</sup>, Milano Maurizio<sup>1</sup>, Pelosi Nicola<sup>1</sup>, Punzo Michele<sup>1</sup>, Tarallo Daniela<sup>1</sup>, Massarotti Nicola<sup>3</sup>

<sup>1</sup>Consiglio Nazionale delle Ricerche. Calata porta di Massa, int. Porto, 80133 Napoli Italy;

<sup>2</sup>Università degli Studi di Napoli Federico II, via Claudio 21, 80125 Napoli Italy;

<sup>3</sup>Università degli Studi di Napoli Parthenope, Centro Direzionale, Isola C4 80143, Napoli, Italy;

marina.iorio@cnr.it

**Keywords:** Exploration, geophysics, hydro-chemic, low-middle enthalpy exploitation, Volcanic.

### ABSTRACT

The active volcanic area of Campi Flegrei caldera (CFc) has been the site of many geothermal investigations, since the early XX century. However, all investigations were concentrated in the western and northern sector of the geothermal system, for its characteristic of medium-high enthalpy resources. Only recently the hypothesized favorable characteristics of the eastern sector reservoir (liquid phase and almost neutral pH values) with respect to the one of the central sectors (gas dominated and acid pH values), despite the lower temperatures, allow an increasing interest in the exploration of this sector of geothermal field. So far, the Agnano caldera has been studied through the research project GeoGrid. Preliminary results from a seismic, geo-electric, gravimetric, hydro-chemical and groundwater data surveys reveal a groundwater flow from NE to SW, in full agreement with the data of scientific literature. Along the flow direction, the chemism and temperature of groundwater present discontinuous manifestations of thermal waters rich in CO<sub>2</sub>, suggesting that the local fresh groundwater receives endogenous inputs (even at high temperatures) of CO<sub>2</sub> well correlated to important tectonic lines identified by geophysical and stratigraphic data. In future these findings could be utilised for sustainability analysis of low-middle enthalpy resource exploitation of the area.

### 1. INTRODUCTION

The Campi Flegrei caldera (CFc) is a large active volcanic complex lying in the Campanian Plain, Southern Italy. Its central-eastern sector, presently experiencing bradyseism and intense swarm seismicity episodes, is extensively studied and monitored. (e.g. Buono et al., 2022). Formation and development of

calderas are accompanied by hydrothermal activity, hot fluids circulation and mineralization processes. Deformation and fracturing, produced by both explosive volcanic activity (hydro-magmatic) and collapse resurgence processes, increases the permeability of rocks, enhancing the advection of fluids in the shallow crust and generating a high heat mass transport (Ingebritsen et al., 2008). However, since present time, the geothermal resource at CFc has been used just for spa and wellness, and in very few cases for houses heating. Recently, the CFc area presenting characters of low and medium-high enthalpy geothermal systems has been interpreted through a complete conceptual models (Siniscalchi et al., 2019), which delineates the presence of two different geothermal reservoirs: one located in the central sector (Solfatara\_Pisciarelli zone) dominated by highly active vapours generated by episodic arrival of CO<sub>2</sub>-rich magmatic fluids and the other one located in the eastern sector (Agnano zone) characterised by a shallow (400-500 m b.s.l.) still hot reservoir, heated by the upward circulation of deep no-magmatic hot vapour. The hypothesized favorable characteristics of the eastern sector reservoir allow an increasing interest in the exploration of this less known geothermal field. So far, the physiochemical features of the Agnano aquifers and the characteristics of the geothermal reservoir have been preliminary determined through a multidisciplinary work combining seismic, gravimetric, geo-electric, hydro-chemical and groundwater data, obtained through experimental campaigns carried out in the framework of the GeoGrid project (Technologies and Innovative system for sustainability use of geothermal energy, POR Campania FESR 2014-2020) (Figure 1). The integration of our data with previously published geologic subsurface data, provide key information for a better understanding of the structural asset and thermal fluid pathways of the Agnano geothermal reservoir. Finally, due to its proximity to densely populated areas, these findings, a crucial task to assess

the economic feasibility of the geothermal exploitation and the development of future project plants (Carotenuto et al., 2016, Calise et al., 2018, Iorio et al., 2020), could be utilized for sustainability analysis of low-middle enthalpy resource exploitation applied for example to district heating and cooling of buildings.

## 2. GEOLOGICAL CONTEXT

The CFc volcanic complex hosted in the metropolitan area of Naples, (Southern Italy) (Figure 1) is constituted by two concentric segmented caldera rings (Tramelli et al., 2006, Acocella, 2010;) and characterised by graben-like structures and volcanic deposits, mainly due to the eruptions of Campania Ignimbrite (CI) (about 40 ky; Gebauer et al., 2014) and Neapolitan Yellow Tuff (NYT) (about 15 ky; Deino et al., 2004). Plio-Quaternary continental and marine sediments fill the caldera with a thickness from 2000 to 3000 m. Actually, after a long period of subsidence, the CFc shows signs of potential reactivation characterised by episodes of ground uplift, shallow seismicity, significant increase in hydrothermal degassing and changes in fluid-geochemistry. The seismicity recorded since 2000 is very shallow and highly concentrated below the Solfatara crater (Tramelli et al., 2021). In the renewed area of seismic activity, the phreatic Pisciarelli field shows the opening of new vents and a significant increase of flow rates and temperatures of existing fumaroles (Chiodini et al., 2016). Today the amount of the diffusively released CO<sub>2</sub> (up to 3000 t/d, Cardellini et al., 2017) is that of a persistently degassing active volcanoes. However, moving towards the eastern side, the hydrothermal activity in the center of the Agnano crater, is different with respect to the ones in Solfatara-Pisciarelli district, being mostly characterized by thermal waters discharge rather than gas. (Vaselli et al 2011. Siniscalchi et al., 2019). The CFc volcanic activity in the last 15 ka was concentrated inside the NYT caldera and stratigraphic markers as well-recognizable volcanic units (i.e. Monte S. Angelo, Agnano\_Monte Spina, Astroni Tephra), paleosols and absolute age dating were used from exposed and cored sequences to build up a chronostratigraphic sequence history. So far, the volcanic activity was subdivided in three epochs (from ~15.0 to 10.5, ~9.6 to 9.1 ~5.5 to 3.8 ka, respectively), (e.g. Di Vito et al., 1999, Smith et al., 2011, Bevilacqua et al., 2016) separated by two mature and widely distributed paleosols. Except for four lava units, complex pyroclastic sequences, produced by mostly explosive monogenetic volcanic activity, are the main characteristic of the about 70 volcanic units recognized through outcrop and borehole sequences (Di Vito et al., 1999, De Vita et al., 1999, Smith et al., 2011). The Agnano plain, located in the northeastern sector of CFc, was generated during the third period of CFc activity, by a volcano-tectonic collapse affecting an area of about 6 km<sup>2</sup> related to the ~ 4400 years BP Agnano–Monte Spina eruption (Di Vito et al., 1999, De Vita et al., 1999 Smith et al.,

2011). The collapse was preceded by fracturing of the vent area and occurred through variable episodes of sinking. Both fracturing and sinking episodes determined vent migration and affected the dynamics of the magma reservoir. The collapsed area was delimited by NE–SW and NW–SE faults that likely resulted from partial reactivation of old faults. The net vertical displacement during collapse was 35 m. The Agnano plain continued to subside at least until the Astroni eruption, which occurred at about 3800 years BP., and the actual plain shape takes into account this northwestern volcano apparatus. (De Vita et al., 1999). Main informations about the stratigraphic sequence unit present in the subsoil of Agnano plain derive from the interpretation of a borehole, located in the southern sector, which shows an alternance of deposits attributed to Costa S., Damiano, Monte S. Angelo, Agnano\_Monte Spina and Astroni tephra, intercalated by marine and palustrine sediments. (Di Vito et al., 1999).

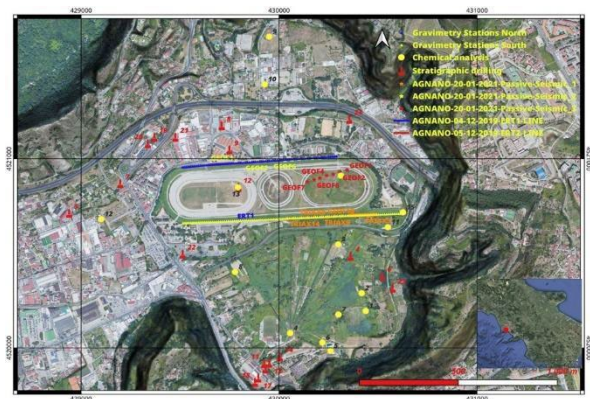


**Figure 1: Localization of all collected data**

### 2.1 Electrical Resistivity Tomography (ERT)

Electrical Resistivity Tomography (ERT) consists in the experimental determination of the apparent resistivity,  $\rho$ , by means of joint measurements of electric current intensity and voltage introduced into the subsoil through electrodes, driven in the ground surface. By deploying a linear array of dipoles, and recording the electrical signals, it is possible to back-figure a 2D pseudo-section, which can be subsequently turned into an actual resistivity section. The resistivity distribution can be interpreted in terms of soil lithology and degree of saturation, taking into account that  $\rho$  increases with grain size, cementation and moisture content. The theories and applications of 2D ERT technique to monitor geothermal site (Drahor et al., 2014; De Giorgi and Leucci, 2015) are well established. Electrical resistivity data were generated along three profiles collected in the Agnano Hippodrome (AH from here) (Figure 1) using an IRIS Syscal-Pro 96-node imaging system with stainless-steel electrodes. The profiles were obtained using the Schlumberger reciprocal array to allow for a high in-depth resolution while maintaining the degree of sensitivity to horizontal changes in resistivity. Electrode coordinates were obtained using a real-time kinematic Global Positioning System (GPS) with 2 cm

accuracy. The resistivity, which was directly measured in the field survey, is not the true resistivity of the subsurface, but an “apparent” resistivity value. To determine the true subsurface resistivity, an inversion of the measured apparent resistivity values was

performed after Loke and Barker (1996a, 1996b). A calculated model of the pseudo-section from the inverted model and the Root Mean Square (RMS) error between the calculated and the measured pseudo-section are obtained from the inversion process .

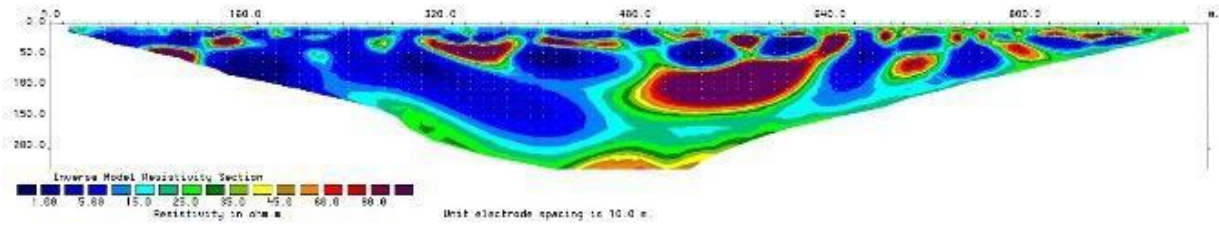


**Figure 2: ERT profile 1 of Agnano Hippodrome**

The interpreted models (example in Figure 2), are then considered as a representation of “true” resistivity of the subsurface, when a close match is made between the modelled resistivity profile and the apparent resistivity inversion profile. The ERT survey allows us to identify the main structural boundaries (and their associated fluid circulations) defining the shallow architecture of the Agnano caldera. The hydrothermal system is identified by very low values of the electrical resistivity (<20 Ωm), while the area with resistivity values up to 80 Ωm could correspond to the presence of pyroclastic fragments. The alternation between low and high resistivity areas could indicate the presence of structures that favour the rise of hydrothermal fluids.

### 3.2 Gravimetric data

Two gravimetric profiles were carried out at the same electrode coordinates (see paragraph 3.1). We acquired gravity data using a Scintrex CG5 AUTOGRAV gravity-meter, which has a standard resolution of 1 μGal with a standard deviation of < 5 μGals. The data have been firstly processed to obtain the complete Bouguer anomalies under usual corrections (e.g. Milsom and Eriksen, 2013) and terrain correction has been calculated using the Oasis Montaj software and a high resolution DTM, out to 200 km from each gravity station. In Figure 3 we show the complete Bouguer anomalies of the profile South (Figure 3a) and North (Figure 3b), respectively. The profile South (1100 m) shows a maximum amplitude of 0.3 mGal with three main highs at around 150 m, 600 m and 1000 m x-distances, while the profile North (780 m) shows mainly a large high with a peak at about 300 m. We investigate the depth, shape and density contrast of the subsurface structures by the CompactDEXP (CDEXP) method (Baniamerian et al., 2016, Liu et al., 2020). The source model is improved iteratively to reconstruct a geologically feasible distribution of source, by implementing a compacting function, based on the estimated model at the previous iteration:

$$W_i = 1 + \frac{\Omega_{i-1}^2}{\sigma^2} [1]$$

where  $\Omega_i$  is the density model obtained at the  $(i-1)^{th}$  iteration, and  $\sigma$  is a positive-value parameter with the same dimension as physical property that controls the degree of compactness or focusing.

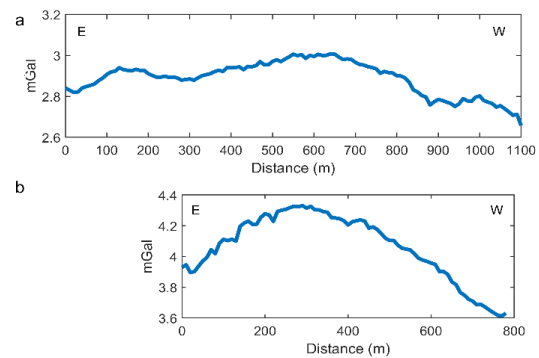


**Figure 3: a) Bouguer gravity anomalies along profile South; b) Bouguer gravity anomalies along profile North.**

The CDEXP imaging was performed on the 1<sup>st</sup> order vertical gradient of the gravity field of profiles North and South, to model the main subsurface structures below the AH. In Figure 4 we show the obtained density models and the computed gravity gradient anomalies vs. the observed anomalies for the south profile.

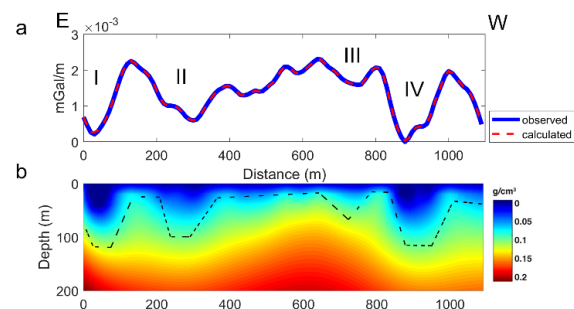


**Figure 4: CDEXP analysis results. a) Observed**

**and calculated vertical gradient data along profile South; b) Density model obtained from the CDEXP analysis along profile south. Black dashed lines represent the interpreted structural features.**

The model mostly shows an interface with a complex morphology separating two layers with different rock density and reaching a maximum density contrast  $> 0.2 \text{ g/cm}^3$  at around 200 m depth. The interface structures, qualitatively indicated with black dashed lines in Figure 4, develops as horst, almost up to the ground level, and graben that on the eastern and western sides are bordered by sub-vertical structural elements (I and IV in Figure 4a). By comparing these results with the resistivity model of Figure 2 along the southern gravimetric profile, we observe a good correspondence between the main gravimetric anomalies with the main resistivity paths probably indicating the rise of hydrothermal fluids along structural limits.

### 3.2 Seismic passive tomography data

Traditional approaches to surface seismic prospecting involve the use of "active source" methods such as reflection and refraction; an alternative method is to use "natural" microtremors (usually considered "noise" in traditional seismic investigations), as a source of surface wave energy. These passive techniques are based on the measurement and analysis of ground vibrations induced by uncontrolled sources, or on the study of the so-called "environmental seismic noise" (displacements of the order of  $10^4$ - $10^2$  mm). The measurements of single-station microtremors, also known as the Nakamura test (1989) or HVSr (Horizontal to Vertical Spectral Ratio) technique, try to retrieve information of seismic impedance contrasts in the subsoil, that are responsible for seismic resonance phenomena, which appears as a peak,  $f_0$ , in the HVSr curve (Kramer 1996). The noise recordings were acquired with triaxial geophones (GS-ONE LF) (location in Figure 1), all oriented according to a common reference (magnetic north pole) (The tool has the following features: Frequency:  $4.5 \text{ Hz} \pm 0.75 \text{ Hz}$ , Coil resistance:  $2450 \text{ Ohm} \pm 5\%$ ; Sensitivity:  $89.4 \text{ V/m/s}$ ; Moving Mass:  $25.2 \text{ g}$ ; Weight:  $131 \text{ g}$ ). The noise data were amplified and digitized using 24-bit GEODE seismographs and acquired at the sampling frequency of  $125 \text{ Hz}$ . The overall duration of the recording, for each profile, was over 60 minutes, thus producing a robust estimates of the environmental vibrations field. HVSr analyses consist of 35 free-field measurements taken on an approximate  $0.15 \text{ Km}^2$  area; after processing the frequencies of the HVSr, peaks determined at each point were used to contour the iso-frequency, showing the  $f_0$  of the overburden (Figure 5). The peaks frequency ranges from  $2.4$  to  $8.5 \text{ Hz}$ . The transition between higher and lower frequencies zone is clear; this limit is located almost in the hippodrome middle; there is, in fact, a strong difference in impedance contrast between the north-western and south-eastern area of the study area

suggesting a thicker sedimentary cover and a deeper seismic bedrock, moving from north-west to south-east

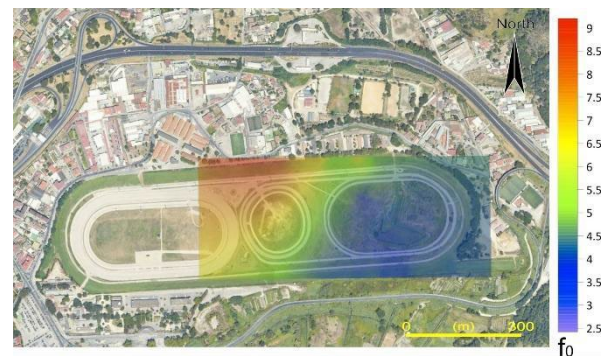


**Figure 5: Orthophoto image (from GoogleEarth) with superimposition of the contour map of the fundamental frequency peak ( $f_0$ ) derived from HVSr analysis of microtremor data**

### 3.4 Stratigraphic data

In the Agnano plain, 20 sedimentary records of variables depths ( $-20$  to  $-107 \text{ m}$ ), from wells drilled in the last 50 years, were analyzed and two of them (Wells 12 and 4, Figure 1) were considered the most useful for our geophysical interpretations analysis. For well 12 it was found that the uppermost  $25 \text{ m}$  consists of loose sand. The subsequent  $78 \text{ m}$  are constituted by lavas deposits, while the depths from  $103$  to  $105 \text{ m}$  are characterized by clay sediments. In well 4, instead, the uppermost  $5 \text{ m}$  consists of palustrine deposits below that we found  $32 \text{ m}$  of rather compact sandy pyroclastic deposits, while from  $37$  to  $93 \text{ m}$  an alternating of different size pyroclastic deposits with lavas fragments is observed. Finally, from  $93$  to  $98 \text{ m}$  trachytic lavas are recovered. It was found that the most interesting characteristic of wells 12 and 4 for our geophysical analysis is the different recovering depths of lavas deposits ( $-25$  and  $-98 \text{ m}$  respectively). Based on the chronostratigraphy of volcanic events reconstructed by Di Vito et al., (1999), Smith et al., (2011), and on the correlation between well 4 and the close (about  $200 \text{ m}$ ) well 46 (Di Vito et al., 1999), whose stratigraphic volcanic units were related to known CFC eruption events, it is thought that the recovered lava deposits in well 12 and 4 are, probably, belonging to the Monte Spina lavas event.

### 3.5 Geochemical Data

The survey of the groundwater level in 15 wells (Figure 1 and 6) shows the presence of a unique groundwater body for the concordance of water levels in wells of various depths (Corniello and Nicotera 1981, De Vita et al., 2018). The groundwater contour lines have a strong flexion due to the drainage exerted on the groundwater. Physico-chemical analyses were performed in almost all the water points of Figure 6. The main results are in Table 1 in which the waters were brought in homogeneous groups. Of particular

interest are the waters of the south-eastern sector where there is also a thermal spring (De Pisis,  $T > 50^{\circ}\text{C}$ ). The chemism of these waters, and mostly of the spring, is due to the important fault that probably limits this sector of the caldera (De Vita et al., 1999). It is likely that along this fault high temperature gases (essentially  $\text{CO}_2$ ) rise up, increasing the reactivity of the groundwater towards the reservoir rock. Due to the proximity of the zone of interest to the sea, the rising of deep gases would also bring seawater (or deeper brine) in fresh groundwater (Figure 7).

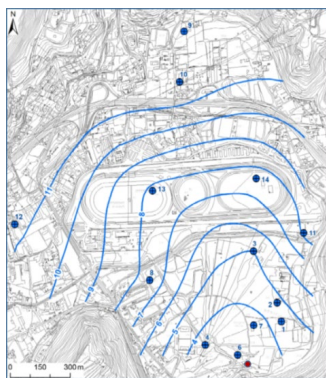


**Figure 6: Groundwater contour lines (in m a.s.l.; June-July 2021). The red dot indicates the De Pisis spring (n° 5 Table 1).**

N.	T °C	pH	TDS		CO <sub>2</sub>	Cl	SO <sub>4</sub>	Na	K	Ca	Mg	NO <sub>3</sub>
			mg/L	mg/L	mg/L	mg/L	mg/L	mg/L	mg/L	mg/L	mg/L	mg/L
1	24,5	6,7	1864,0	68,7	448,0	191,0	419,0	150,0	118,0	34,6	2,9	
2	25,6	6,7	1957,0	247,0	473,0	160,0	444,0	127,0	133,0	27,6	2,9	
3	25,1	6,9	1567,0	395,0	363,0	184,0	385,0	102,0	125,0	21,7	2,9	
6	26,7	6,5	1845,0	149,0	393,0	24,1	439,0	126,0	119,0	28,4	< 1	
7	26,5	6,5	1548,0	450,0	285,0	183,0	415,0	97,4	109,0	26,5	2,9	
15	28,5	7,1	1520,0	217,0	354,0	154,0	317,0	89,0	118,0	17,8	2,4	
9	24,4	6,9	1185,0	364,0	140,0	258,0	260,0	71,2	109,0	16,7	2,1	
10	24,5	7,0	654,0	321,0	56,9	69,2	111,0	40,8	70,0	10,6	76,6	
11	19,5	7,1	845,0	279,0	112,0	244,0	126,0	71,3	95,3	13,6	< 1	
12	27,0	7,5	996,0	279,0	147,0	183,0	151,0	115,0	124,0	17,3	218,0	
14	22,0	7,2	850,0	488,0	87,3	210,0	157,0	61,9	91,9	13,4	20,9	
8	27,3	6,7	1508,0	664,0	216,0	146,0	422,0	87,6	133,0	26,6	1,8	
13	39,0	6,9	2842,0	487,0	436,0	240,0	874,0	114,0	117,0	44,5	4,4	
5*	57,0	6,3	7450,0		2910,0	282,0	2064,0	257,0	257,0	73,0		

**Table 1: Physico-chemical data of more significant groundwater in Figure 1. The analysis of De Pisis spring (n°5) is from Valentino and Stanzone 2004 (analysis of 1994) and from Venturini et al., 2017; the values in the last column are in meq**

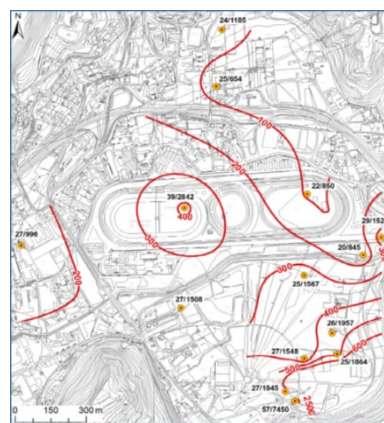


**Figure 7: Cl contour lines (mg/L); T (°C) / TDS (mg/L)**

#### 4. COMPARISON OF GEOPHYSICAL STRATIGRAPHIC AND GEOCHEMICAL DATA BY MEAN OF GEOGRID VIEWER SOFTWARE

A 3D subsoil model of a sector of Agnano caldera was developed by mean of “Geogrid viewer”, an application specially developed during the GeoGrid project to allow operators to view multi-parameter data in interactive three-dimensional graph format. In our study the model utilizes the joint interpretation of gravimetric, geo-electric and seismic data, integrated with stratigraphy data of wells 12 and 4, together with 10 water samples of which the temperature, conductivity and hydrogen carbonate values are major of  $25.1^{\circ}\text{C}$ ,  $2000\ \mu\text{S}/\text{cm}$  and  $600\ \text{mg}/\text{L}$ . In figure 8 it is possible to notice the correspondence among identified depths of main density contrasts interfaces and different lithology boundaries in the south gravimetric profiles and well 4. In particular low-density values occupy the most superficial sector down to about -40 meters, and are interpreted based on the well stratigraphy as marsh and loose sandy pyroclastic deposits (Blue color in both gravimetric profile and well). Below this formation, higher density contrast values from  $0.07$  to  $0.15\ \text{g}/\text{cm}^3$  have a strictly correspondence with different sizes pyroclastic sediments and lava fragments sedimentary unit of well 4 down to -93 m. (Heavenly-light green colors in both gravimetric profile and well). Highest density contrast values (up to  $0.2\ \text{g}/\text{cm}^3$ ) corresponding to lavas deposits, were intercepted in well 4 from -93 to -98 m, (Yellow colors in both gravimetric profile and well). It was found that a complex morphology of the subsoil is present, showing in the first 200 m a general lowering of higher density body towards south and south-east. This finding is confirmed by the seismic bedrock surface trend obtained by seismic data.

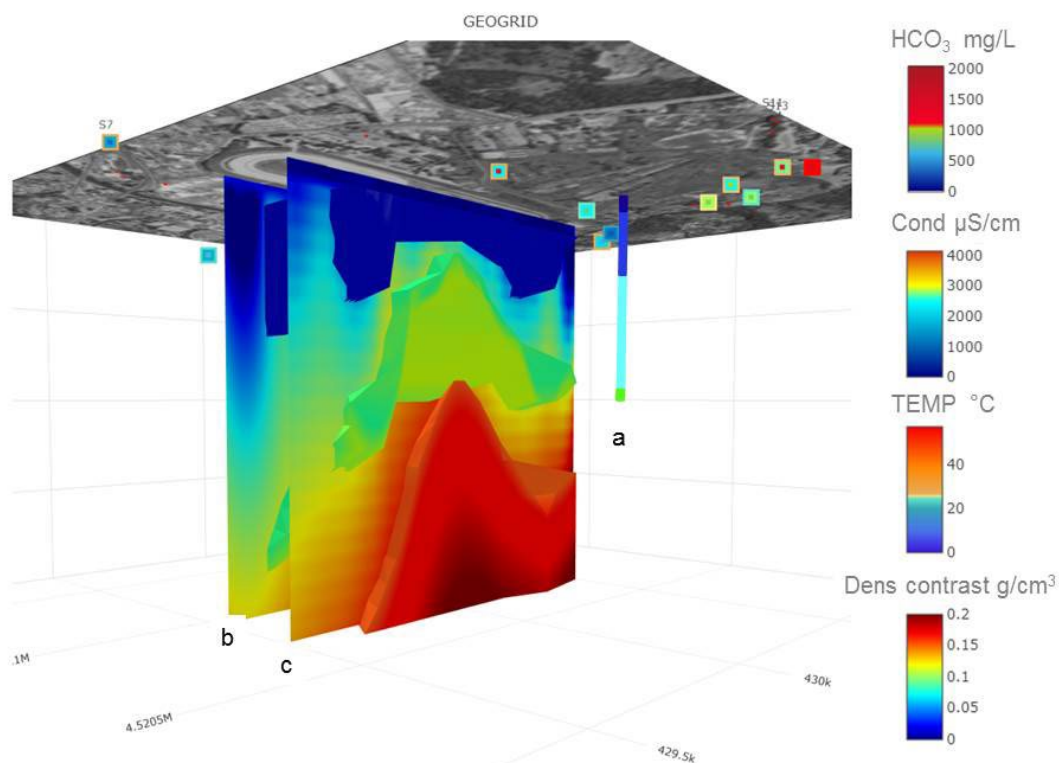


**Figure 8: 3D subsoil representation of gravimetric, seismic, stratigraphic and geochemical data. Temperature, conductivity and hydrogen carbonate contents are indicated by large, middle and little squares, respectively. a stratigraphic log of well 4 (see text for color meanings), b and c North and South gravimetric profiles respectively.**

## 5. CONCLUSIONS

A detailed reconstruction of the main geophysical and geological-structural properties of a sector of Agnano caldera have been obtained by means of gravimetric, geoelectric and geochemical data acquired as part of the GeoGrid project. The first interpretative phases of the acquired data show how the gravimetric anomalies along both profiles can be mainly associated with structural elements previously only hypothesized by geological studies. Density contrast and coincident resistivity changes were also analyzed for a better interpretation of structural elements and thermal fluid circulation. A preliminary three-dimensional representation of the results obtained was provided thanks to the use of the Geogrid Viewer software, which, using the previously developed model and integrating additional information from well surveys, made it possible to interpret the geometry and development of the main lithological interfaces of the underground in three dimensions. Moreover, the structural processes that have strongly characterized the subsoil of the AH are in good agreement with the seismic bedrock trend detected by a passive seismic

survey, while the geochemical data extended to the entire basin confirm the structural control on the rising of gases and fluids from the depths. Finally, these results will be of interest for further sustainability and economic feasibility analysis of low-middle enthalpy resource exploitation for a sector of Agnano caldera characterized by a large quantity of mineralized waters, not enriched by sea water contribution.

## REFERENCES

- Acocella, V. Evaluating fracture patterns within a resurgent caldera: Campi Flegrei, Italy. *Bulletin of Volcanology*, **72(5)**, (2010), 623–638. <https://doi.org/10.1007/s00445-010-0347-x>
- Baniamerian, J., Fedi, M., and Oskooi, B.: Research Note: Compact Depth from Extreme Points: a tool for fast potential field imaging. *Geophysical Prospecting*, **64(5)**, (2016), 1386–1398.
- Bevilacqua, A., Flandoli, F., Neri, A., Isaia, R., and Vitale, S. Temporal models for the episodic volcanism of Campi Flegrei caldera (Italy) with uncertainty quantification. *Journal of Geophysical Research: Solid Earth*, **121**, (2016), 7821–7845. <https://doi.org/10.1002/2016JB013171>
- Buono, G., Paonita, A., Pappalardo, L., Caliro, S., Tramelli, A., and Chiodini, G. New insights into

- the recent magma dynamics under Campi Flegrei caldera (Italy) from petrological and geochemical evidence. *Journal of Geophysical Research: Solid Earth*, **127**, (2022), e2021JB023773. <https://doi.org/10.1029/2021JB023773>
- Calise, F., Di Fraia, S., Macaluso, A., Massarotti, N., Vanoli, L.: A geothermal energy system for wastewater sludge drying and electricity production in a small island. *Energy* **163**, (2018), 130–143.
- Cardellini, C., Chiodini, G., Frondini, F., Avino, R., Bagnato, E., Caliro, S., et al. Monitoring diffuse volcanic degassing during volcanic unrests: The case of Campi Flegrei (Italy). *Scientific Reports*, **7(1)**, (2017), 6757. <https://doi.org/10.1038/s41598-017-06941-2>
- Carotenuto, A., De Luca, G., Fabozzi, S., Figaj, R. D., Iorio, M., Massarotti, N., Vanoli, L.: Energy Analysis of a Small Geothermal District Heating System in Southern Italy. *International Journal of Heat and Technology*, **34(2)**, (2016) S519-S527.
- Chiodini, G., Paonita, A., Aiuppa, A., Costa, A., Caliro, S., De Martino, P., et al. Magmas near the critical degassing pressure drive volcanic unrest towards a critical state. *Nature Communications*, **7(1)**, (2016), 13712. <https://doi.org/10.1038/ncomms13712>
- Corniello, A. and Nicotera, P.: Geologia, idrogeologia e idro-chimica della zona sud-occidentale dei Campi Flegrei. *Memorie e Note Istituto di Geologia Applicata*, **16**, (1982), Napoli.
- De Giorgi, L., Leucci, G.: Study of Shallow Low-Enthalpy Geothermal Resources Using Integrated Geophysical Methods. *Acta Geophys.* **63**, 2015125–153. <https://doi.org/10.2478/s11600-014-0243-4>
- Deino, A. L., Orsi, G., de Vita, S., and Piochi, M.: The age of the Neapolitan Yellow Tuff caldera-forming eruption (Campi Flegrei caldera -Italy) assessed by  $^{40}\text{Ar}/^{39}\text{Ar}$  dating method. *Journal of Volcanology and Geothermal Research*, **133**, (2004), 157–170. [https://doi.org/10.1016/S0377-0273\(03\)00396-2](https://doi.org/10.1016/S0377-0273(03)00396-2)
- Drahor, M.G., Berge, M.A., Bakak, Ö., Öztürk, C.: Electrical resistivity tomography monitoring studies at Balçova (Turkey) geothermal site. *Near Surface Geophysics*, **12**, (2014), 337-350.
- De Vita, S., Orsi g., Civetta L., Carandente A., D'Antonio M., Deino A., Di Cesare T., Di Vito M., Fisher R.V., Isaia R., Marotta E., Necco A., Ort M., Pappalardo L., Piochi M., Southon J.: The Agnano Monte Spina eruption (4100 years BP) in the restless Campi Flegrei caldera (Italy). *J. Volcanol. Geotherm. Res.*, **91**, (1999), 269-301.
- De Vita, P., Allocca, V., Celico, F., Fabbrocino, S., Mattia, C., Monacelli, G., Musilli I., Piscopo, V., Scalise, A.R., Summa, G., Tranfaglia, G., Celico, P.: Hydrogeology of continental southern Italy. *J. Maps*, **14 (2)** (2018), pp. 230-241.
- Di Fraia, S., Macaluso, A., Massarotti, N., Vanoli, L.: Energy, exergy and economic analysis of a novel geothermal energy system for wastewater and sludge treatment. *Energy Convers. Manag.*, **195**, (2019), 533–547, [doi:10.1016/j.enconman.2019.05.035](https://doi.org/10.1016/j.enconman.2019.05.035).
- Di Vito, M. A., Isaia, R., Orsi, G., Southon, J., De Vita, S., D'Antonio, M., Pappalardo, L., and Piochi M.: Volcanism and deformation since 12,000 years at the Campi Flegrei caldera (Italy), *J. Volcanol. Geotherm. Res.*, **91**, (1999), 221–246.
- Gebauer, S. K., Schmitt, A. K., Pappalardo, L., Stockli, D. F., and Lovera, O. M.: Crystallization and eruption ages of Breccia Museo (Campi Flegrei caldera, Italy) plutonic clasts and their relation to the Campanian ignimbrite. *Contributions to Mineralogy and Petrology*, **167**, (2014). 1–18. <https://doi.org/10.1007/s00410-013-0953-7>
- Ingebritsen, S., Sanford, W., Neuzil, C.: *Groundwater in Geological Processes*, Cambridge. (2008).
- Iorio M., Carotenuto, A., Corniello, A., Di Fraia, S., Massarotti, N., Mauro, A., Somma, R., Vanoli, L.: Low Enthalpy Geothermal System in Structural Controlled Areas: A sustainability Analysis of Geothermal Resources for Heating Plant (The Mondragone Case in Southern Appennines, Italy) *Energies*, **13 (5)**, (2020), 1237. [https://DOI: 10.3390/en13051237](https://DOI:10.3390/en13051237)
- Kramer, S.L., *Geotechnical earthquake engineering. Prentice Hall Inc*, New Jersey, p 653, (1996).
- Liu, S., Baniamerian, J., and Fedi, M.: Imaging Methods Versus Inverse Methods: An Option or An Alternative? *IEEE Transactions on Geoscience and Remote Sensing: A Publication of the IEEE Geoscience and Remote Sensing Society*, **58(5)**, (2020), 3484–3494.
- Loke M.H. and Barker, R.D.: Rapid Least-Squares Inversion of Apparent Resistivity Pseudosections by a Quasi-Newton Method. *Geophysical Prospecting*, **44**, (1996a), 131-152. <http://dx.doi.org/10.1111/j.1365-2478.1996.tb00142.x>.
- Loke M.H. and Barker R.D.: Practical techniques for 3D resistivity surveys and data inversion. *Geophysical Prospecting*, **44**, Issue 3, (1996b), 499-523. <https://doi.org/10.1111/j.1365-2478.1996.tb00162.x>.
- Nakamura, Y.: A method for dynamic characteristics estimation of subsurface using microtremor on the ground surface. *Quarterly Report of RTRI, Railway Technical Research Institute (RTRI) vol. 30*, no 1, (1989), pp 25–30.

- Siniscalchi, A., Tripaldi, S., Romano, G., Chiodini, G., Improta, L., Petrillo, Z., et al. Reservoir structure and hydraulic properties of the Campi Flegrei geothermal system inferred by audiomagnetotelluric, geochemical, and seismicity study. *Journal of Geophysical Research: Solid Earth*, **124**, (2019), 5336–5356. doi:10.1029/2018JB016514
- Smith, V. C., Isaia, R., and Pearce N. J. G.: Tephrostratigraphy and glass compositions of post-15 ka Campi Flegrei eruptions: Implications for eruption history and chronostratigraphic markers, *Quat. Sci. Rev.*, **30**, (2011), 3638–3660.
- Tramelli, A., Del Pezzo, E., Bianco, F., and Boschi, E. 3D scattering image of the Campi Flegrei caldera (Southern Italy): New hints on the position of the old caldera rim. *Physics of the Earth and Planetary Interiors*, **155(3-4)**, (2006), 269–280. <https://doi.org/10.1016/j.pepi.2005.12.009>
- Tramelli, A., Godano, C., Ricciolino, P., Giudicepietro, F., Caliro, S., Orazi, M., et al.: Statistics of seismicity to Investigate the campi flegrei caldera unrest. *Scientific Reports*, **11**, (2021), 1. <https://doi.org/10.1038/s41598-021-86506-6>
- Valentino, G.M. and Stanzione, D.: Geochemical monitoring of the thermal waters of Phlegraean Fields. *Journal of Volcanology and Geothermal Research*, **133**, (2004), 261-289.
- Vaselli, O., Tassi, F., Tedesco, D., Poreda, J. R., and Caprai, A.: Submarine and inland gas discharges from the Campi Flegrei (southern Italy) and the Pozzuoli Bay: Geochemical clues for a common hydrothermal-magmatic source. *Procedia Earth and Planetary Science*, **4**, (2011), 57–73.
- Venturi, S., Tassi, F., Bicocchi, G., Cabassi, J., Capechciacci, F., Capasso, G., Vaselli, O., Ricci, A. and Fausto Grassa, F.: Fractionation processes affecting the stable carbon isotope signature of thermal waters from hydrothermal/volcanic systems: The examples of Campi Flegrei and Vulcano Island (southern Italy). *Journal of Volcanology and Geothermal Research*, **345**, (2017), 46-57.